Diamagnetic Susceptibility Obtained from the Six-Vertex Model and Its Implications for the High-Temperature Diamagnetic State of Cuprate Superconductors

Jay D. Sau and Sumanta Tewari

Phys. Rev. Lett. **107**, 177006 — Published 20 October 2011

DOI: 10.1103/PhysRevLett.107.177006

Diamagnetic susceptibility obtained from the six-vertex model and its implications for the high-temperature diamagnetic state of cuprate superconductors

Jay D. Sau[1*] and Sumanta Tewari[2]
[1]*Condensed Matter Theory Center and Joint Quantum Institute, Department of Physics, University of Maryland, College Park, Maryland 20742-4111, USA*
[2]*Department of Physics and Astronomy, Clemson University, Clemson, SC 29634*

We study the diamagnetism of the 6-vertex model with the arrows as directed bond currents. To our knowledge, this is the first study of the diamagnetism of this model. A special version of this model, called F model, describes the thermal disordering transition of an orbital antiferromagnet, known as d-density wave (DDW), a proposed state for the pseudogap phase of the high-T_c cuprates. We find that the F model is strongly diamagnetic and the susceptibility may diverge in the high temperature critical phase with power law arrow correlations. These results may explain the surprising recent observation of a diverging low-field diamagnetic susceptibility seen in some optimally doped cuprates within the DDW model of the pseudogap phase.

PACS numbers: 73.43.Nq,74.25.Dw,75.10.Hk

Introduction. Experiments on the normal state properties of the cuprate superconductors continue to pose new theoretical challenges. Above the superconducting transition temperature T_c, the cuprates in the underdoped regime evince a d-wave-like gap even in the absence of superconductivity. The nature of the system in this pseudogap phase is believed to hold the key [1] to the physics of the high transition temperature itself. A recent remarkable set of experiments [2, 3] have found evidence of enhanced diamagnetism in the pseudogap phase above T_c at a doping range near and below the optimal doping. In particular, these experiments have revealed that, near optimal doping, the low-field diamagnetic susceptibility χ *diverges* above T_c as an inverse power of the applied field H, $\chi \sim -H^{-x}$. Here x is a T-dependent exponent. The divergence of χ above T_c implies underlying critical correlations in an entire phase above T_c [2] which is not easy to explain by any existing theories of the pseudogap phase [2, 3]. In this paper, we will address this question within the framework of the d-density wave (DDW) state [4], which was proposed [5] as a candidate state responsible for the many anomalous properties of the pseudogap phase. Our results on diamagnetism will also be important in light of the recent experiments in Ref. [6] which point towards an alternative source different from vortices to explain the large diamagnetism observed in the pseudogap state of the cuprates.

The ordered DDW state consists of counter propagating bond currents on the neighboring plaquettes of a 2D square lattice (Fig. 1) [4], which can be taken as the Cu lattice of the high-T_c cuprates [5]. The diamagnetism of this state has already been examined within a mean field description [7] in which the direction of the currents on the bonds remains frozen. The only source of diamagnetism in this description are the nodal quasiparticles, whose contribution has been shown to be exceedingly small [7]. However, the mean field description does not include the *direction fluctuations* of the bond currents themselves. Because fluctuating bond currents respond much more strongly than quasiparticles to an applied magnetic field (see below), it is possible that these fluctuations gives rise to an enhanced diamagnetic response. A suitable way to include these direction fluctuations is to formulate the DDW state in terms of a vertex model, in which the directed arrows represent directed bond currents (Fig. 1). In this paper we use this vertex model description of the DDW state to show that the diamagnetism of the state significantly enhances with increasing temperatures. Further, including also the magnitude fluctuations of the bond currents (not contained in the usual 6-vertex model), which are important at high temperatures, we show that the high-T, low-field, χ can diverge as a power law of the applied field H.

6-vertex model and F-model The classical vertex models were originally proposed to study anti-ferroelectric materials and associated phase transitions in electric fields [9, 10]. One specific vertex model, called the 6-vertex model, is particularly interesting since it can be solved exactly by transfer matrices [8, 11, 12]. The 6-vertex model is defined by a set of vertices constructed out of directed arrow variables defined on the bonds of a square lattice. The arrows can represent any directed classical variable which serves as the building block of a thermodynamic statistical mechanical system. To describe an orbital current system the arrows are taken as directed bond currents. On the 2D $x-y$ plane, each of the nearest-neighbor bonds in the 4 directions $\boldsymbol{d} = \pm a\hat{x}, \pm a\hat{y}$ from a vertex v is associated with an orbital current $I_v^{(\boldsymbol{d})}$ of magnitude I_0. The current $I_v^{(\boldsymbol{d})}$ is positive for current flowing parallel to $\boldsymbol{d}$ and negative for current flowing anti-parallel to $\boldsymbol{d}$. In the steady state, there is no charge accumulation at each vertex and therefore the current is divergence-free ($\sum_{\boldsymbol{d}} I_v^{(\boldsymbol{d})} = 0$). This mandates that the total number of possible vertices on a square lattice is $\frac{4!}{2!2!} = 6$ (Fig. 1). The Hamiltonian describing the orientation of the currents for a special case of the 6-vertex model called F model ([9, 11])is given by

$$H_0 = \sum_{v,\boldsymbol{d}} -\frac{K}{2}(I_v^{(\boldsymbol{d})} - I_v^{(-\boldsymbol{d})})^2. \quad (1)$$

As is clear from Eq. 1, in the F-model the anti-ferroelectric (AF) vertices (defined by $I_v^{\hat{x}} = -I_v^{-\hat{x}}$ and $I_v^{\hat{y}} = -I_v^{-\hat{y}}$) are assigned negative energies $-K$ and the rest of the vertices

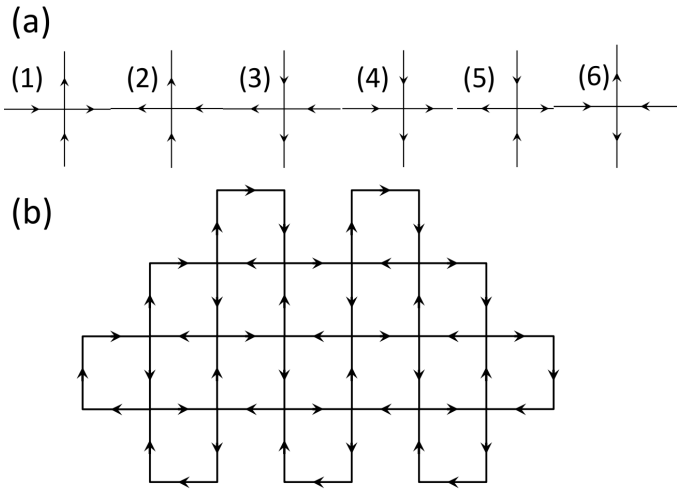

FIG. 1. (a) The six possible current vertices in the 6-vertex model. The vertices (5) and (6) are the AF vertices energetically favored by the F model. (b) The AF aligned low-temperature ground state of the F model corresponds to the $d-$density wave (DDW) state proposed for the cuprate superconductors.

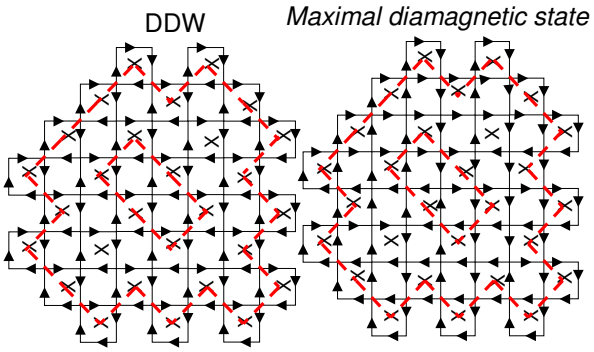

FIG. 2. (Color online) Two states, AF and the maximally current carrying state l of the 6-vertex model. The AF state is characterized by small clock-wise loops around plaquettes on one of the sublattices (marked by X). To construct the maximally current carrying state l, one starts with the AF state and reverses the counter-clockwise currents adjacent to all closed loops (red dashed curves). See text for details.

have energy 0. Therefore, at low T, the ground state of the F-model is the ordered AF state, which is nothing but the ordered DDW state when the arrows represent currents. The AF state survives thermal fluctuations up to a critical temperature $T = T^*$. Above T^* the current variables disorder into a critical phase with power-law current correlations [8].

DDW state and its relevance to the high-T_c cuprates. The singlet DDW state, described by an order parameter $\left\langle \hat{c}^\dagger_{\boldsymbol{k}+\boldsymbol{Q},\alpha}\hat{c}_{\boldsymbol{k},\beta}\right\rangle \propto iW_{\boldsymbol{k}}\,\delta_{\alpha\beta},\ W_{\boldsymbol{k}} = \frac{W_0}{2}(\cos k_x - \cos k_y)$, $\hat{c}_{\boldsymbol{k}}, \hat{c}^\dagger_{\boldsymbol{k}}$ are fermion operators, $\boldsymbol{k}$ is a 2D momentum, $\boldsymbol{Q} = (\pi,\pi)$, and α,β are spin indices, has been proposed as providing a phenomenologically consistent explanation for the pseudogap phase of the underdoped cuprates [5]. The assumption of DDW order below optimal doping can lead to an explanation of numerous experiments including the abrupt suppression of the superfluid density [13] and Hall number [14] below optimal doping as well as the more recent quantum oscillation experiments [15] and Nernst effect [16]. Mathematically, any Hamiltonian that leads to d-wave superconductivity in the underdoped cuprates will almost certainly favor DDW order as well [4, 17], making their coexistence and competition in the phase diagram a plausible scenario.

Connection of DDW state with F-model. In a mean field picture, the only way the DDW state can thermally disorder is via a collapse of the magnitude of the order parameter W_0 (i.e. collapse of the magnitudes of the currents themselves) at a second order thermal phase transition. However, this mean field description does not take into account the possible direction fluctuations of the bond currents. As is clear from Fig. 1, the ordered DDW state is nothing but the low-T AF state of the F model. In F model, with increase in T, the direction fluctuations of the currents eventually make the system pass into a current disordered state above the temperature T^*. Thus the DDW state can thermally disorder by bond current fluctuations above T^* long before the order parameter magnitude W_0 itself collapses at a mean-field temperature $T_m > T^*$. In this way the F-model and its quantum extension have recently been used [18, 19] to describe the thermal and quantum disordering transitions of the DDW state in the underdoped regime of the cuprates.

Diamagnetic response of F-model. Let us first give an intuitive argument for the diamagnetism of the F-model. The interaction of the orbital currents with an external magnetic field can be described by a term $H_{mag} = -\int d\boldsymbol{r}\boldsymbol{J}(\boldsymbol{r})\cdot\boldsymbol{A}(\boldsymbol{r})$ where $\boldsymbol{J}(\boldsymbol{r})$ is the orbital current density and $\boldsymbol{A}(\boldsymbol{r})$ is the vector potential. The expression for H_{mag} is derived by applying the minimal substitution $\boldsymbol{p} \to (\boldsymbol{p} - q\boldsymbol{A}/c)$ to the Schrodinger equation for the electrons. The divergenceless orbital current $\boldsymbol{J}(\boldsymbol{r})$ can be expressed in terms of a magnetization density $\boldsymbol{m}(\boldsymbol{r})$, $\boldsymbol{J}(\boldsymbol{r}) = \boldsymbol{\nabla}\times\boldsymbol{m}(\boldsymbol{r})$. Using the vector magnetic field $\boldsymbol{B} = \boldsymbol{\nabla}\times\boldsymbol{A}$ and integration by parts lead to the form $H_{mag} = -\int d\boldsymbol{r}\boldsymbol{J}(\boldsymbol{r})\cdot\boldsymbol{A}(\boldsymbol{r}) = \int d\boldsymbol{r}\boldsymbol{m}(\boldsymbol{r})\cdot\boldsymbol{B}$. Thus, the bond currents can lower energy by aligning in circles perpendicular to $\boldsymbol{B}$ so that $\boldsymbol{B}\cdot\boldsymbol{m}(\boldsymbol{r}) < 0$ (hence the response is diamagnetic). If such an arrangement of bond currents can be accessed by flipping the local vertices in closed loops (to maintain the charge conservation)(Fig. 2), the resultant diamagnetic response can be large . Below we discuss this more quantitatively.

Adding the magnetic interaction term H_{mag} to the Hamiltonian in Eq. 1 we get the total Hamiltonian as:

$$H = \sum_{v,\boldsymbol{d}}[-\frac{K}{2}(I_v^{(\boldsymbol{d})} - I_v^{(-\boldsymbol{d})})^2 - aI_v^{(\boldsymbol{d})}\boldsymbol{d}\cdot\boldsymbol{A}(v+\frac{\boldsymbol{d}}{2})]. \quad (2)$$

Here $\boldsymbol{A}(x,y)$ is the vector potential given by $\boldsymbol{A}(x,y) = \frac{1}{2}(-By, Bx)$. The second term is equivalent to H_{mag} when the current densities are limited to the bonds and is equivalent to $\boldsymbol{B}\cdot\boldsymbol{M}$ where $\boldsymbol{M}$ is the total magnetic moment. To cal-

culate the magnetization density we write the partition function $Z = \sum_j e^{-E_j/k_BT} = e^{-E_0/k_BT} + \sum_{j\neq 0} e^{-E_j/k_BT} = e^{-E_0/k_BT}[1+\sum_{j\neq 0} e^{-(E_j-E_0)/k_BT}]$, where E_j is the energy associated with the configuration j and $j=0$ is the minimum energy configuration. Using Eq. 2, the energy E_j is given by $E_j = E_j^v + \boldsymbol{B}\cdot\boldsymbol{M}_j$ where E_j^v is the energy of the first term of H and $\boldsymbol{M}_j$ is the total magnetic moment of configuration j. Calling the configuration with the maximum diamagnetic moment l (Fig. 2 right panel), the free-energy $F = -k_BT\log Z$ can be written as

$$F = \boldsymbol{B}\cdot\boldsymbol{M}_l + \tilde{E}_0 - k_BT\log\left[1+\sum_{j\neq 0} e^{-\frac{(E_j-E_0)}{k_BT}}\right] \quad (3)$$

where $\tilde{E}_j = E_j^v + \boldsymbol{B}\cdot[\boldsymbol{M}_j - \boldsymbol{M}_l]$ and $\tilde{E}_0 = \min_j \tilde{E}_j$. Since $\tilde{E}_0 \leq \tilde{E}_l = E_l^v$ and $\boldsymbol{B}\cdot\boldsymbol{M}_0 \geq \boldsymbol{B}\cdot\boldsymbol{M}_l$, it follows that $E_0^v \leq \tilde{E}_0 \leq E_l^v$. Additionally, the magnitude of the energy E_j^v of any state j from Eq. 1 must be less than $KI_0^2R^2$ where R is the radius of the system containing $\sim R^2$ vertices. Thus the second term $\tilde{E}_0$ is bounded by $|\tilde{E}_0| \leq KI_0^2R^2$. The third term in Eq. 3 which is logarithmic also scales as R^2 since each of the terms under the summation over j is less than unity and there are at most 6^{R^2} such terms corresponding to the current configurations on R^2 vertices. Combining these results, we find that

$$F = BM_l + \mathcal{O}(R^2) \quad (4)$$

where $\mathcal{O}(R^2)$ represents corrections of order R^2 (which can be neglected as $|\boldsymbol{M}_l| \sim I_0R^3/a$ as we show below).

The state l with maximum diamagnetic moment is understood by starting with the AF state as follows (Fig. 2): Imagine large closed loops (red dashed curves) passing through the dual lattice points marked by the crosses. The currents on the bonds touching these loops but on the two opposite sides flow in opposite directions. For example, on the left panel of Fig. 2, the bond currents right outside the loops are clockwise and right inside are counter-clockwise. Reversing the counter-clockwise currents touching all such closed loops leads to the state l shown on the right panel. The total magnetization M is the product of the current and the total area enclosed by all the clockwise loops. Since most of the clockwise loops ($\sim R/a$ in number) enclose an area of order R^2, the total magnetic moment is $\boldsymbol{M}_l \propto -\hat{z}I_0R^3/a$ which is the desired result. Using this equation for M_l and neglecting terms of $\mathcal{O}(R^2)$ for large R we get from Eqn. 4, $F(B) = -BI_0R^3/a$. The magnetization density is calculated as $\boldsymbol{m}(B) = \frac{\hat{z}}{R^2}\frac{\partial F}{\partial B}$. This gives $m(B) \sim -\hat{z}I_0R/a$, which is divergent in the thermodynamic limit ($R\to\infty$) for any non-vanishing B.

So far we have ignored the magnetic field generated by the induced currents themselves. Such a field results in a magnetostatic current-current interaction. The current-current interaction can be accounted for by using simple magnetostatics,

$$H = B + 4\pi|\boldsymbol{m}(B)|, \quad (5)$$

where B is the magnetic field and H is the magnetic induction which can be taken as the externally applied magnetic field. Here $\boldsymbol{m}(B)$ is the magnetization density which is opposite in direction to B (diamagnetic) in sign and increases in magnitude from $|\boldsymbol{m}(B)| = 0$ at $B = 0$ to $|\boldsymbol{m}(B)| \sim I_0R/a$ for any magnetic field $B \gtrsim \mathcal{O}(1/R)$. To estimate the solution B of Eq. 5 let us define the function $f(B) = B + 4\pi|\boldsymbol{m}(B)| - H$ such that Eq. 5 is written as $f(B) = 0$. Since $H < I_0R/a$ ($R\to\infty$ in the thermodynamic limit), it follows that $f(B) > 0$ for $B \gtrsim \mathcal{O}(1/R)$. On the other hand $f(B=0) = -H < 0$. Therefore $f(B)$, being an increasing function of B, has a unique root satisfying the constraint $B \lesssim \mathcal{O}(1/R)$. Since in the thermodynamic limit $R\to\infty$, it follows that B is completely expelled from the system and it behaves like a perfect diamagnet similar to a type I superconductor.

Diamagnetism in the AF phase. Despite the above analysis, the low-T ($T \ll T^*$) AF phase being gapped is not expected to have a large diamagnetic response. The response of the AF phase to a magnetic field should be dominated by flips of small current loops. The combination of these elementary current loop flips can generate a flip of a large loop of length L which has a magnetic moment $|\boldsymbol{M}| \sim I_0L^2$. From Eq. 1 such loop flips cost energy KL (flipping each AF vertex costs energy K and L such vertices need to be flipped for a loop of length L). However, the applied field lowers the energy of such a current loop by $-B|\boldsymbol{M}| = -BI_0L^2$. Thus the energy cost of a flipped loop, $V(L) = KL - BI_0L^2$, is positive for small L, has a positive peak at $L = K/2BI_0$ and becomes negative for large L. Thus only loops that form out of a thermal fluctuation with an energy larger than $\max_L V(L) = K^2/2BI_0$ can cross the threshold value of $L = K/2BI_0$ to become a large loop. The fraction of such high energy loops is determined by the Boltzmann factor as $e^{-K^2/2k_BTBI_0}$. Thus the AF state is stable for low-T and B (i.e $e^{-K^2/2k_BTBI_0} \ll 1$). This conclusion is also consistent with the numerical monte-carlo simulations [23]. It also follows that as T increases (T is a substantial fraction of T^*), the diamagnetic response of the AF state should increase significantly. However, the time-scale for development of diamagnetic response is expected to become longer as temperature becomes smaller than T^* leading to possible hysteretic behavior of the magnetization as a function of applied magnetic field.

Diamagnetism in the critical phase. For $T > T^*$, the AF order is completely destroyed and the system develops critical current fluctuations whose correlation is scale-invariant. From the argument in the previous paragraph it follows that this phase is strongly diamagnetic. The scale invariance of the fluctuations in the critical phase allows one to describe the critical phase by a continuum theory such as a height model [21, 22]. In the height model the magnetization density $\boldsymbol{m}(\boldsymbol{r})$ is mapped to the vertical displacement $h(\boldsymbol{r})$ of a $2D$ surface such that $\boldsymbol{m}(\boldsymbol{r}) = I_0h(\boldsymbol{r})\hat{z}$ and $\boldsymbol{J}(\boldsymbol{r}) = \boldsymbol{\nabla}\times\boldsymbol{m}(\boldsymbol{r})$.

The current-current correlations in the high T critical phase of the F model are obtained from the Gaussian theory of height fluctuations [21, 22] described by the coarse-grained contin-

uum Hamiltonian

$$H = \int d^2\boldsymbol{r}\tilde{K}|\nabla h|^2 - \boldsymbol{B}\cdot\boldsymbol{M}_{tot} \quad (6)$$

where $\boldsymbol{M}_{tot}$ as before is the total magnetization of the model.

From the argument in the last section, it is clear that for $T \gtrsim T^*$, the F model responds to a magnetic field by generating large current loops. This results in the formation of patches of circulating currents. If the sizes of these patches are macroscopically large, this would lead to perfect diamagnetism. However, so far we have neglected the *magnitude* fluctuations of the bond currents I_0, which should be taken into account at high T. Such magnitude fluctuations of I_0 can occur from spontaneous thermal fluctuations of the DDW gap magnitude W_0 and variations of the local density of quasiparticles. Here by quasiparticles we mean the quasiparticles in the DDW state that carry charge [24]. In the presence of such magnitude fluctuations the bond-current I_0 is allowed to vary spatially as $I_0(\boldsymbol{r},t)$ so that the current density is now given by $\boldsymbol{J}(\boldsymbol{r},t) = I_0(\boldsymbol{r},t)\boldsymbol{\nabla}\times(h(\boldsymbol{r})\hat{\boldsymbol{z}})$. Therefore it is no longer a divergence-free quantity. The magnitude fluctuations of the currents will lead to a cut-off length-scale $R_0 > R_p$ for the patch sizes R_p. The introduction of this cut-off length-scale in the original F model directly leads to a power-law dependence of m on B as we show at the end of this section. Below we first speculate on a possible mechanism for the emergence of this cut-off scale.

Let us consider a patch with a circularly symmetric current density $\boldsymbol{J}(\boldsymbol{r},t) = I_0(\boldsymbol{r},t)(\boldsymbol{\nabla}h(r)\times\hat{\boldsymbol{z}}) = I_0(\boldsymbol{r},t)h'(r)\hat{\boldsymbol{\theta}}$ corresponding to a circularly symmetric height profile $h(r)$. Apart from a thermal fluctuation component, $\zeta(\boldsymbol{r},t)$, the magnitude of the local current $I_0(\boldsymbol{r},t)$ depends on the density of quasiparticles $n(\boldsymbol{r},t)$. Writing $I_0(\boldsymbol{r},t) = I_0(S(n(\boldsymbol{r},t)) + \zeta(\boldsymbol{r},t))$, the time-varying current density $\boldsymbol{J}(\boldsymbol{r},t)$ is now given by $\boldsymbol{J}(\boldsymbol{r},t) = I_0(\boldsymbol{r},t)h'(r)\hat{\boldsymbol{\theta}} = I_0h'(r)[S(n(\boldsymbol{r},t) + \hat{\boldsymbol{\theta}}\cdot\boldsymbol{\nabla}\zeta(\boldsymbol{r},t)]\hat{\boldsymbol{\theta}} = J(r)[S(n(\boldsymbol{r},t))+\hat{\boldsymbol{\theta}}\cdot\boldsymbol{\nabla}\zeta(\boldsymbol{r},t)]\hat{\boldsymbol{\theta}}$, where $h'(r) = \frac{dh(r)}{dr}$, $\zeta(\boldsymbol{r},t)$ is the noise term that accounts for the spontaneous thermal fluctuations of the current density and $\hat{\boldsymbol{\theta}}$ is the tangential direction around a loop on the circular patch. Since charge density is conserved we have the continuity equation, $\partial_t n(\boldsymbol{r},t) + \boldsymbol{\nabla}\cdot\boldsymbol{J}(n(\boldsymbol{r},t)) = D\nabla^2 n$, where D is the diffusion constant of the quasiparticles. For a circular profile of a single patch of circulating currents, this equation can be written as

$$\partial_t n + J(r)[S'(n)\hat{\boldsymbol{\theta}}\cdot\boldsymbol{\nabla}n + \hat{\boldsymbol{\theta}}\cdot\boldsymbol{\nabla}\zeta(\boldsymbol{r},t)] = D\nabla^2 n. \quad (7)$$

The second term in the above equation, which is referred to as the bond-current term drives current only along the tangential direction to the loop at a given radius and hence is one-dimensional in character. The quasiparticle diffusion term on the right hand side of the above equation is two dimensional in space and in general will have a finite radial component. However, long wave-length fluctuations in the bond current $\zeta(\boldsymbol{r},t)$ (the correlation function of $\zeta(\boldsymbol{r},t)$ is taken as $\langle\zeta(\boldsymbol{r},t)\zeta(\boldsymbol{r}',t')\rangle \sim \delta(\boldsymbol{r}-\boldsymbol{r}')\delta(t-t')$), with a length-scale λ, create long wave-length variations in the quasiparticle density which are tangential in direction (as shown by the third term in Eq. 7). The evolution of the quasiparticle density following such a fluctuation, which is described by Eq. 7, is dominated by the tangential bond-current term (i.e. second term), which scales as λ^{-1}, and the contribution of the radial diffusion term (which scales as λ^{-2}) is subdominant for large λ. Therefore, the long length-scale behavior of Eq. 7 can be understood in terms of approximately decoupled 1D conservation law equations for each loop at radii $|\boldsymbol{r}| = r$. As shown in Refs. [25, 26, 28], for mean-field bond-current densities $S(n)$ which vanish for very small or large quasiparticle densities, such 1D equations are unstable to the proliferation of long-lived shock solutions and the current density I_0 is expected to drop to zero at some radius R_0 which can be determined by solving the relation $J(r = R_0) \propto R_0^{-\alpha}$. In the present case, how such a relation arises can be seen in the following way. From Eq. 7, we see that the bond-current term at a length-scale R_0 scales as $J(r = R_0)R_0^{-1}$, while the diffusion term scales as DR_0^{-2}. Thus the bond-current term, which drives the instability, dominates at a radius R_0 when $J(r = R_0)R_0^{-1} \sim DR_0^{-2}$. This leads to the constraint $J(r = R_0) \propto R_0^{-\alpha}$ with $\alpha = 1$. In reality this simple argument ignores the R_0-dependence of n_s [25, 27], which leads to a value of α slightly greater than 1.

Let us now return to the F model and show that the introduction of a cut-off scale leads to a power-law dependence of m on B. We consider the free-energy of a patch of finite radius R_0. Using Eq. 6 the free-energy density of such a patch is given by

$$f = \int_0^{R_0} \frac{2rdr}{R_0^2}(\tilde{K}h'^2 - I_0Bh). \quad (8)$$

Minimizing f with respect to h using the usual method of variations (and without any approximations) leads to $h'(r) = -BI_0r/4\tilde{K}$. Using the relation $I_0h'(R_0) = R_0^{-\alpha}$, we get $R_0 \propto B^{-1/(1+\alpha)}$. Substituting this in Eq. 8 leads to $f \propto B^2R_0^2 \sim B^{2\alpha/(1+\alpha)}$. The diamagnetic susceptibility $\chi = \frac{\partial^2 f}{\partial B^2} \propto B^{-2/(1+\alpha)}$ diverges as an inverse power-law.

Conclusion. We analyze the diamagnetic response of the 6-vertex model, which is used to model the DDW phase proposed for the pseudo-gap phase of the high-T_c cuprates. We find that deep in the low-T AF phase the diamagnetic response is weak. With increasing T, especially for $T \lesssim T^*$, the diamagnetism is significantly enhanced. The disordered critical phase for $T > T^*$, is perfectly diamagnetic within the strict 6-vertex model. With the magnitude fluctuations of the current (magnitude fluctuations of the DDW order parameter W_0) taken into account, the low-field diamagnetic susceptibility χ in this phase diverges as a power-law of the field.

We thank S. Chakravarty for pointing out a crucial error in an earlier version of the manuscript. We also thank J. Toner and N. P. Armitage for valuable discussions. We acknowledge the hospitality of the Aspen Center for Physics where part of this work was completed. Sau acknowledges DARPA-QuEST and JQI-NSF-PFC, and Tewari acknowledges DARPA MTO Grant No:FA9550-10-1-0497 for support.

* Present Address: Department of Physics, Harvard University, Cambridge, MA 02138.

[1] M. R. Norman, D. Pines, C. Kallin, Adv. Phys. **54**, 715 (2005).
[2] L. Li *et al.*, Phys. Rev. B **81**, 054510 (2010).
[3] S. A. Kivelson, E. Fradkin, Physics **3**, 15 (2010)
[4] C. Nayak, Phys. Rev. B **62**, 4880 (2000).
[5] S. Chakravarty *et al.*, Phys. Rev. B **63**, 094503 (2001).
[6] L.S. Bilbro *et al.*, arXiv:1103.2402v1 (2011).
[7] A. Ghosal, P. Goswami, S. Chakravarty, Phys. Rev. B **75**, 115123 (2007).
[8] R. Baxter, *Exactly Solvable Models in Statistical Mechanics*, Academic Press (2004).
[9] F. Rys, Helv. Phys. Acta,**36**, 537 (1963).
[10] J. F. Nagle, J. Math. Phys, **7**,1492 (1966).
[11] E. H. Lieb, Phys. Rev. Lett.,**18**, 1046 (1967).
[12] E. H. Lieb, Phys. Rev. Lett.,**18**, 692 (1967).
[13] S. Tewari, H.-Y. Kee, C. Nayak, and S. Chakravarty, Phys. Rev. B **64**, 224516 (2001).
[14] S. Chakravarty, C. Nayak, S. Tewari, and X. Yang, Phys. Rev. Lett. **89**, 277003 (2002).
[15] S. Chakravarty and H.-Y. Kee, Proc. Natl. Acad. Sci. USA **105**, 8835 (2008).
[16] S. Tewari, C. W. Zhang, Phys. Rev. Lett. **103**, 077001 (2009); C. W. Zhang *et al.*, Phys. Rev. B **81**, 104517 (2010)
[17] C. Nayak and E. Pivovarov, Phys. Rev. B **66**, 064508 (2002).
[18] S. Chakravarty, Phys. Rev. B **66**, 224505 (2002).
[19] O. F. Syljuasen, S. Chakravarty, Phys. Rev. Lett. **96**, 147004 (2006).
[20] C. P. Yang, Phys. Rev. Lett. 19, 586(1967).
[21] H. Beijeren, Phys. Rev. Lett. **38**:993 (1977).
[22] J. Kondev and C.L. Henley, Nucl. Phys. B, **464**, 540 (1996).
[23] A. V. Kpadonou, F. Hontinfinde, Physica A, **362**,345 (2006).
[24] S. Chakravarty, C. Nayak, S. Tewari,Phys. Rev. B, **68**, 100504(R) (2003).
[25] G.B. Whitham, Linear and nonlinear waves, Wiley Interscience (1999).
[26] H. Beijeren, R. Kutner, H. Spohn, Phys. Rev. Lett, **54**,2026 (1985).
[27] H. Fogedby, A. Brandenburg, Phys. Rev. E, **66**, 016604 (2002).
[28] H. Jensen, Physica Scripta, **43**,593 (1991).